

# Identification of Thyroid Cancerous Nodule using Local Binary Pattern Variants in Ultrasound Images

Nanda S<sup>1</sup>, M Sukumar<sup>2</sup>

<sup>1</sup> Research Scholar, JSS Research Foundation, Sri Jayachamarajendra College of Engineering, Mysuru, Karnataka, India

<sup>2</sup> Research Guide, JSS Research Foundation, Sri Jayachamarajendra College of Engineering, Mysuru, Karnataka, India

**Abstract:** Most of the thyroid nodules are heterogeneous in nature with dissimilar echo patterns. Hence texture characterization plays a major role in discriminating benign and malignant nodules in thyroid ultrasound images. This paper addresses the classification of thyroid nodule through local binary pattern (LBP), local configuration pattern (LCP) and completed local binary pattern (CLBP) variants. This work comprises of 60 thyroid ultrasound images. LBP, LCP and CLBP features are extracted from the thyroid images. These features are used to train and test support vector machine (SVM). Accuracy, sensitivity, specificity, positive predictive value and negative predictive values are calculated. Performances of the classifier with linear, polynomial and radial basis function (RBF) kernels are compared. Best accuracy of 94.5% has been achieved when CLBP features are given to SVM of different forms.

**Keywords** — Completed local binary pattern, Local binary pattern, Local configuration pattern, Thyroid nodule.

## I. INTRODUCTION

Thyroid cancer is common in women and in the elderly population. First sign of thyroid cancer is a thyroid nodule. A lump will be formed if there is an abnormal growth in the cells within thyroid gland. Identification of malignancy risk factor of thyroid nodule is the major challenge [1] and is useful in avoiding unnecessary and costly invasive procedures. Ultrasound imaging is the popular, non invasive and cost effective modality in evaluating the thyroid nodule. Ultrasound images of benign and malignant thyroid nodules have discernible sonographic characteristics. The shape of the malignant nodule is more composite than benign nodule due to their invade characteristics into surrounding tissues. Precise visual interpretation of these images can only be done by radiologists with lot of experience and training. Otherwise it results in subjective interpretation and inter-observer variabilities. These limitations have led to the research in developing

computer aided diagnosis (CAD) system to obtain accurate and more objective diagnosis results. In the past decades extensive study has been done by the researchers on numerous feature extraction approaches for texture characterization. Representative methods include textural features, morphological features, wavelet based features, Gabor features and fractal dimension [1],[2],[3],[4] to characterize thyroid nodules. The use of LBP variants as texture descriptors for medical images is discussed by Lorriss et al. [5],[6]. Sunhua Wan et al. [7] has presented a method for breast tissue classification using spoke LBP and ring LBP features. Mellisa Cote et al. [8] showed the robustness of LBP block based approaches for texture classification. Hence in this study LBP, LCP and CLBP variants are extracted from the thyroid ultrasound images. SVM is used for the differentiation of the nodules. Performances of the classifier with various kernels are compared.

## II. MATERIALS

Digital database of thyroid ultrasound images (DDTI), a public database [9] consists of delineated thyroid nodule images and their pathologies confirmed by fine needle aspiration biopsy. In this study 60 images (30 images consisting of benign nodules and 30 having malignant nodules) are used to evaluate the performances of the methods.

## III. METHODOLOGY

The steps involved in identifying thyroid cancerous nodule are shown in Fig.1. Thyroid ultrasound images are pre processed using anisotropic diffusion filtering and the region of interest (ROI) is extracted from each image. LBP, LCP and CLBP based features are computed from each ROI. These features are given as the input to the classifiers to differentiate benign and malignant nodule.

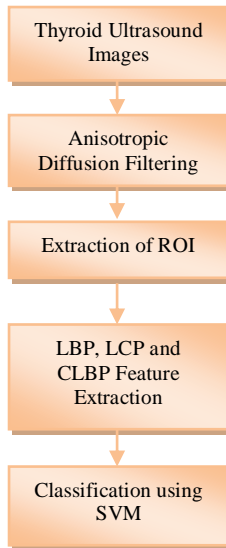


Fig.1: Block diagram of the method

**A. Pre processing**

Ultrasound images are affected by many types of artefacts making it difficult to interpret and obtain quantitative information from them. The most common ultrasound artefact is the speckle noise. Anisotropic diffusion (AD) filter [10] reduces the noise in images by smoothing homogeneous regions without blurring the edges. AD has been widely used for image enhancement in biomedical imaging [11]. Hence in this study anisotropic diffusion is used to enhance thyroid ultrasound images.

**A. Feature Extraction**

Features are the descriptors that are useful in characterizing the image. The aim of feature extraction is to maximize the discriminating performance of the feature group. Feature vectors highly affect the performance of the classification. Thus, the extraction of useful features is a crucial task. In this study LBP, LCP and CLBP features are extracted from the ROI.

**(1) Local Binary Pattern**

LBP is a local texture operator [12] used to represent salient micro patterns in images. It extracts information that is invariant to local gray scale variations in the images. Extraction of LBP consists of thresholding and encoding steps. LBP value of the centre pixel is calculated by comparing centre pixel gray value with its neighbourhood pixel values using the following equations.

$$LBP_{P,R}(x_c, y_c) = \sum_{p=0}^{P-1} s(g_p - g_c) 2^p \quad (1)$$

$$s(x) = \begin{cases} 0, & x < 0 \\ 1, & x \geq 0 \end{cases} \quad (2)$$

where  $g_c$  – centre pixel value  
 $g_p$  – neighbourhood pixel value

P – number of neighbourhood pixels  
 R - radius of the neighbourhood

One of the most disadvantages of LBP is that it gives same LBP code for different structural pattern.

**(2) Local Configuration Pattern (LCP)**

Local configuration pattern [13] encodes the texture pattern based on the combination of local information and the microscopic configuration (MiC) information. Local structure information utilizes LBP while microscopic configuration information is obtained from image configuration and pixel-wise interaction relationships. MiC is designed to extract texture pattern from images. Optimal weights of the neighbouring pixel intensities are estimated to model the image configuration. This helps in reconstructing the centre pixel intensity. The reconstruction error is defined as,

$$E(w_0, \dots, w_{p-1}) = |g_c - \sum_{p=0}^{P-1} w_p g_p| \quad (3)$$

where  $g_c$  and  $g_p$  are values of centre and neighboring pixels,  $w_p$ 's are weights.

Optimal parameter  $W_L$  is calculated using

$$W_L = (V_L^T V_L)^{-1} V_L^T C_L \quad (4)$$

where  $C_L$  is the least square problem and  $V_L$  is the neighbouring pixel intensity.

Rotation invariant features are obtained by

$$H_L(k) = \sum_{p=0}^{P-1} W_L(i) e^{-j2\pi kp/P} \quad (5)$$

Magnitude of  $H_L$  is taken as MiC feature and is defined as,

$$|H_L| = [|H_L(0)|; |H_L(1)|; \dots; |H_L(P-1)|] \quad (6)$$

LCP can be written as,

$$LCP = [ [|H_0|; O_0]; [|H_1|; O_1]; \dots; [|H_{l-1}|; O_{l-1}] ] \quad (7)$$

Where  $l$  is the total number of patterns of interest,  $O_p$  is the  $p^{th}$  local pattern and  $|H_p|$  is calculated using Eq.( 6).

**(3) Completed Local Binary Pattern (CLBP)**

Completed local binary pattern improves the discriminative ability of the local structures [14]. In CLBP the image local differences are divided into two complementary components viz. signs ( $s_p$ ) and magnitudes ( $m_p$ ). This is used to calculate CLBP sign (CLBP\_S), CLBP magnitude (CLBP\_M) and CLBP centre (CLBP\_C). CLBP\_S considers the sign component of the difference between centre pixel and neighbourhood pixel and is same as the conventional LBP sign operator  $s(x)$ . CLBP\_M considers the magnitude component of the difference and is defined as

$$CLBP\_M_{P,R} = \sum_{p=0}^{P-1} t(m_p - c)2^p \quad (8)$$

where threshold  $c$  is the mean value of  $m_p$  of the whole image and  $t(x) = 1$  for  $x \geq 0$ .  
CLBP\_C is defined as

$$CLBP\_C_{P,R} = t(g_c, c1) \quad (9)$$

where  $c1$  is the average image intensity.  
By combining CLBP\_S CLBP\_M and CLBP\_C significant improvement can be observed in differentiating confusing patterns.

### B. Classification

Features that are extracted from the thyroid ultrasound images are given as the input to the classifier to categorize the images into benign and malignant classes. In this work support vector machine (SVM) is used for classification. SVM is basically a powerful two class supervised learning technique. It finds an optimal hyperplane [15] to separate two classes with a margin. Maximum margin in hyperplane results in a good separation between the two classes. The points that lie closest to the hyperplane are support vectors. The optimal hyperplane is completely determined by these support vectors. If the data is linearly separable then SVM produces a hyperplane that separates the data into two non overlapping classes. SVM uses kernel function to map the data into new feature space where a hyperplane (linear) may not be sufficient to do the separation. If the data is not linearly separable then kernel function can be used to transform the data into higher dimensional space to perform the linear separation.

For a two class classification problem the distinguishing function of the non linear SVM is

$$g(x) = \sum_{i=1}^N \alpha_i y_i k(x_i, x_j) + b \quad (10)$$

where  $N$  is the number of training samples,  $x_i$  are the training data belonging to  $y_i \{+1, -1\}$ ,  $\alpha_i$  are the Lagrange multipliers,  $b$  is the bias coefficient and  $k(x_i, x_j)$  is the kernel function.

Frequently used kernels are polynomial, radial basis function (RBF) and sigmoid kernel. In this work polynomial and RBF are used.

Polynomial kernel is described by

$$k(x_i, x_j) = (x_i \cdot x_j + 1)^d \quad (11)$$

where  $d$  is the degree of polynomial.

RBF with Gaussian kernel is given by

$$k(x_i, x_j) = \exp\left[-\frac{(x_i - x_j)^T (x_i - x_j)}{2\sigma^2}\right] \quad (12)$$

where  $\sigma$  is the width of the Gaussian function .

Features extracted from LBP, LCP and CLBP are used to train the classifier. The parameters used to evaluate the performance of the classifier are calculated as follows.

$$Accuracy = \frac{TP+TN}{TP+TN+FP+FN} \times 100 \quad (13)$$

$$Sensitivity = \frac{TP}{TP+FN} \times 100 \quad (14)$$

$$Specificity = \frac{TN}{TN+FP} \times 100 \quad (15)$$

$$Negative Predictive Value (NPV) = \frac{TN}{TN+FN} \times 100 \quad (16)$$

$$Positive Predictive Value (PPV) = \frac{TP}{TP+FP} \times 100 \quad (17)$$

where

TP-True Positive: No. of malignant nodules correctly classified as malignant.

FP-False Positive: No. of benign nodules misclassified as malignant.

TN-True Negative : No. of benign nodules correctly classified as benign.

FN-False Negative: No. of malignant nodules misclassified as benign.

To check the performance of the classification 10 fold cross validation is used in this work. This is repeated ten times and the average results are tabulated.

## IV. RESULTS AND DISCUSSION

Thyroid ultrasound images are obtained from publicly available Digital Database of Thyroid ultrasound Images (DDTI). 30 images consisting of benign nodules and 30 images consisting of malignant nodules are considered. From these images, LBP, LCP and CLBP features are computed. Experimentation has been carried out by considering these features individually as well as with combination. Even though LBP and LCP features are not adequate enough to characterise the texture of the nodule in detail, these features have also been extracted for the purpose of comparative study.

In this study, the extracted features have been classified using the Linear SVM, SVM polynomial kernels of order 1,2,3 and SVM with RBF. Classifications results of Linear SVM is given in Table I and the same has been graphically represented in Fig.2. The results show that CLBP and combination of LCP with CLBP are giving good accuracies of 94.5% and 92.5% respectively.

The features have also been classified using SVM polynomial kernel of order 1, 2 and 3. Since SVM polynomial kernel of order 1 has given good results the same has been tabulated in Table II and its graphical representation is shown in Fig. 3. This classifier has given the best sensitivity of 99.67%.

The results of classification using SVM-RBF is given in Table. III and its graphical representation is

shown in Fig. 4. Overall classification performance of combination of LCP with CLBP is best using this classifier where the sensitivity is 97.25%, specificity is 97% and accuracy is 96%.

TABLE I  
LINEAR SVM PERFORMANCE MEASURES

Performance	Features				
	LBP	LCP	CLBP	LBP+LCP	LCP+CLBP
Accuracy	81.33	85.16	94.50	89.00	92.50
Sensitivity	80.01	86.00	97.25	92.67	97.25
Specificity	89.51	89.00	94.50	87.16	91.50
NPV	74.33	85.00	96.33	92.67	96.33
PPV	88.33	85.33	92.67	85.33	88.67

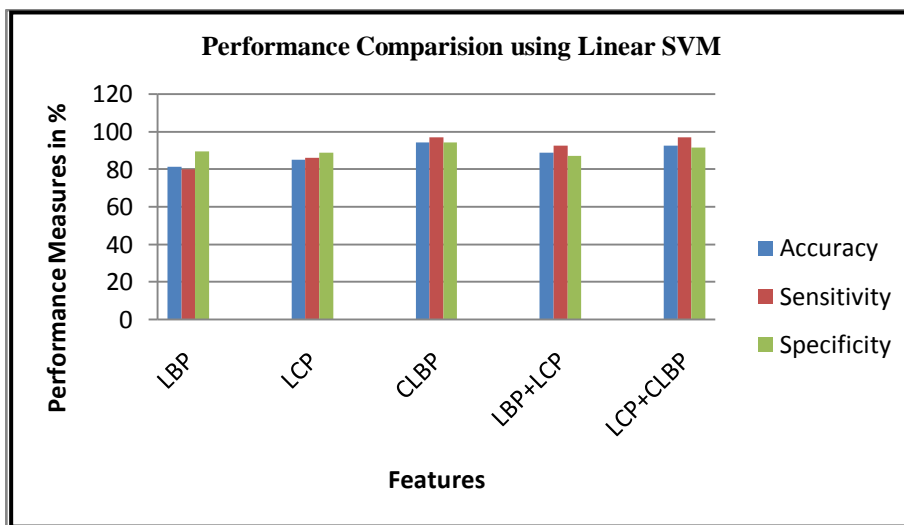


Fig. 2. Performance of Linear SVM

TABLE II  
PERFORMANCE MEASURES SVM – POLYNOMIAL OF DEGREE 1

Performance	Features				
	LBP	LCP	CLBP	LBP+LCP	LCP+CLBP
Accuracy	87.00	92.16	94.50	92.33	94.16
Sensitivity	90.58	96.75	97.25	99.67	99.67
Specificity	88.08	92.35	94.50	88.67	91.41
NPV	88.67	96.00	96.33	99.67	96.67
PPV	85.33	88.33	92.67	85.00	96.00

V. CONCLUSION

Correct identification of cancerous thyroid nodule in ultrasound images through precise characterization is very essential as it can assist the radiologist for accurate diagnosis. This work is focused on the extraction of LBP, LCP and CLBP

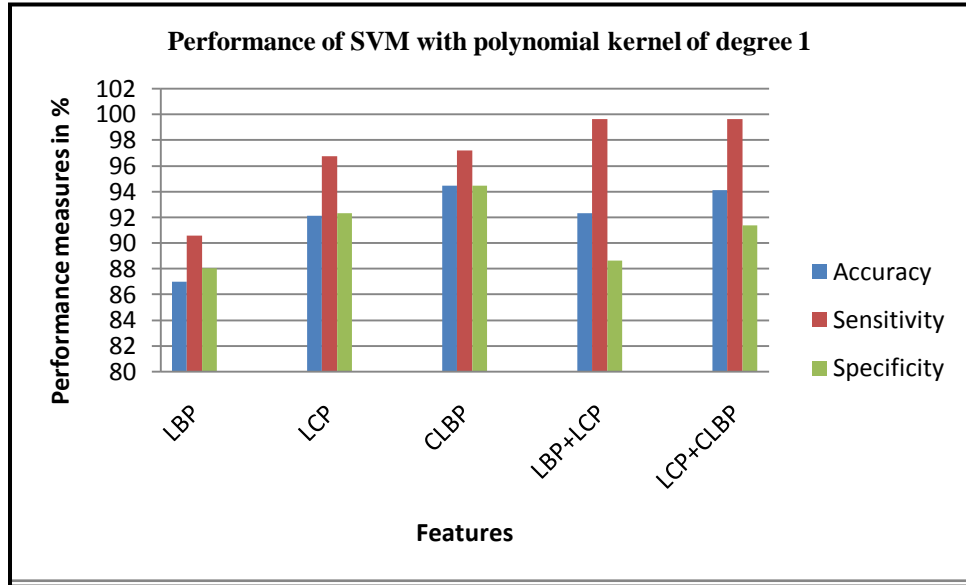


Fig.3. Performance of SVM Polynomial of 1<sup>st</sup> Order

**TABLE III**  
**SVM – RBF PERFORMANCE MEASURES**

Performance	Features				
	LBP	LCP	CLBP	LBP+LCP	LCP+CLBP
Accuracy	83.33	90.67	94.50	87.16	94.16
Sensitivity	84.60	94.50	96.33	95.6	97.25
Specificity	88.75	92.60	93.58	87.35	94.10
NPV	78.00	92.67	96.33	92.67	96.33
PPV	88.67	88.67	92.67	81.67	92.00

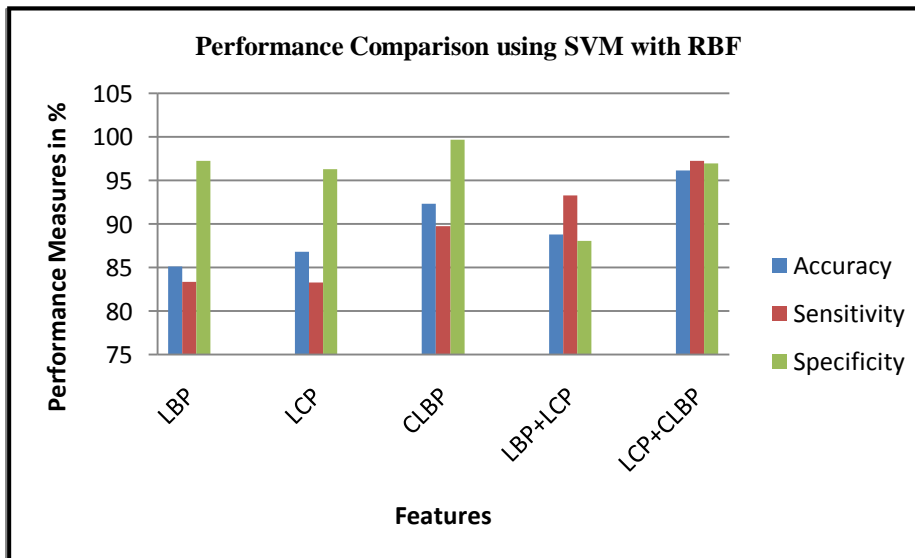


Fig.4. Performance of SVM with RBF

features for the identification of the cancerous nodule using linear SVM, SVM with polynomial kernel of degree 1 and SVM with RBF. A

comparative study has been carried out and classification performances of various forms of SVM are evaluated using all the features extracted.

All the three forms of SVM are giving good accuracy of 94.5% with CLBP features. But the highest sensitivity of 99.67% is obtained by the combination of LCP and CLBP using SVM with polynomial kernel of degree 1. But overall performance is best with combination of LCP and CLBP features classified by SVM – RBF. These promising results encourages us to further explore more discriminative features along with feature vector optimization to improve the classification accuracy.

### REFERENCES

- [1] Stavros Tsantis, Nikos Dimitropoulos, Dionisis Cavouras, George Nikiforidis, "Morphological and wavelet features towards sonographic thyroid nodules evaluation", *Computerized Medical Imaging and Graphics, Elsevier*, vol. 33, no. 2, pp. 91-99, 2009.
- [2] Michalis Savelonas, Dimitris Maroulis, Manolis sangriotis, "A computer aided system for malignancy risk assessment nodules in thyroid US images based on boundary features", *Computer Methods and programs in Biomedicine, Elsevier*, vol. 96, no.1, pp. 25-32, 2009.
- [3] Grigorescu, S. N., Petkov, N., Kruizinga, P. "Comparison of texture features based on Gabor filters", *IEEE Transactions on Image processing*, vol. 11, no. 10, pp. 1160-1167, 2002.
- [4] Yuan Y. Tang, Yu Tao, Ernest C.M. Lam, "New method for feature extraction based on fractal behavior", *Pattern Recognition*, vol. 35, no. 5, pp. 1071–1081, 2002.
- [5] Lorris Nanni, Alessandra Lumini, Sheryl Brahnham, "Local binary patterns variants as texture descriptors for medical image analysis", *Artificial Intelligence in Medicine, Elsevier*, vol. 49, no. 2 pp. 117-125, 2010.
- [6] Lorris Nanni, Alessandra Lumini, Sheryl Brahurveure descriptors for image classification", *Expert Systems with Applications, Elsevier*, vol. 39, no. 3, pp. 3634-3641, 2012.
- [7] Sunhua Wan, Xiaolei Huang, Hsiang Chieh Lee, James G Fujimoto, Chao Zhou, "Spoke-LBP and Ring-LBP:New Texture features for tissue classification", *Pattern Recognition (ICPR) 2016 23rd International Conference on*, pp. 2440-2445, 2016
- [8] Mellisa Cote, Alexandra Branzan Albu, "Robust texture classification by aggregating pixel based LBP statistics", *IEEE Signal Processing Letters*, vol 22,no. 11, pp. 614-618, 2015.
- [9] Lina Pedraza , Carlos Vargas, Fabian Narvaez , Oscar Duran , Em-ma Munoz, Eduardo Romero, "An open access thyroid ultrasound-image database", *Proceedings of SPIE*, Vol. 9287, 2015.
- [10] "P. Perona and J. Malik, "Scale-Space and Edge Detection Using Anisotropic Diffusion", *IEEE Transactions on Pattern Analysis and Machine Intelligence*, vol. 12, no. 7, pp. 629-639, July 1990.
- [11] "G. Grieg, O. Kubler, R. Kikinis, and F. A. Jolesz, "Nonlinear Anisotropic Filtering of MRI Data", *IEEE Transactions on Medical Imaging*, vol. 11, no.2, pp. 221-232, June 1992.
- [12] Ojala T Pietikainen M, Maenpaa T, "Multiresolution gray-scale and rotation invariant texture classification with local binary patterns", *IEEE Transactions on Pattern Analysis and Machine Intelligence* vol. 24, no. 7, pp. 971-987, 2002.
- [13] Y. Guo, G. Zhao, and M. Pietikainen. "Texture Classification using a " Linear Configuration Model based Descriptor" in 22<sup>nd</sup> British Mission Vision Conference , pp. 1-10, Sep. 2011.
- [14] Zhenhua Guo, Lei Zhang, David Jhang, "A completed modeling of local binary pattern operator for texture classification", *IEEE Transactions on Image Processing*, vol. 19, no.6, pp. 1657-1663, June 2010.
- [15] Corinna Cortes, Vladimir Vapnik. "Support-Vector Networks", *Machine Learning*, vol. 20, no. 3, pp. 273-297, 1995.
- [16] T.Saravanan, "Noise Removal In Ultrasound Images", *International Journal of Engineering Trends and Technology (IJETT)*, Vol 3, Issue 2, No. 4, April 2012.
- [17] Suman Pandey, Deepak Kumar Gour, Vivek Sharma, "Comparative Study on Classification of Thyroid Diseases", *International Journal of Engineering Trends and Technology (IJETT)*, Vol 28, No. 9, October 2015.
- [18] Anjali Kapoor, Taranjeet Singh, "Speckle Reducing Filtering for Ultrasound Images", *International Journal of Engineering Trends and Technology (IJETT)*, Vol 37, No. 5, July 2016